# Importance of intertidal sediment processes and porewater exchange on the water column biogeochemistry in a pristine mangrove creek (Ras Dege, Tanzania)

S. Bouillon, J. J. Middelburg, F. Dehairs, A. V. Borges, G. Abril, M. R. Flindt, S. Ulomi, E. Kristensen

Biogeosciences Discuss., 4, 317–348, 2007
www.biogeosciences-discuss.net/4/317/2007/


Biogeosciences Discussions

*Biogeosciences Discussions* is the access reviewed discussion forum of *Biogeosciences*

# Importance of intertidal sediment processes and porewater exchange on the water column biogeochemistry in a pristine mangrove creek (Ras Dege, Tanzania)

**S. Bouillon[1,2], J. J. Middelburg[2], F. Dehairs[1], A. V. Borges[3], G. Abril[4], M. R. Flindt[5], S. Ulomi[5,6], and E. Kristensen[5]**

[1]Vrije Universiteit Brussel, Dept. of Analytical and Environmental Chemistry, Pleinlaan 2, 1050 Brussels, Belgium
[2]Netherlands Institute of Ecology, Centre for Estuarine and Marine Ecology (NIOO-KNAW), Yerseke, The Netherlands
[3]Université de Liège, Chemical Oceanography Unit, Institut de Physique (B5), 4000 Liège, Belgium
[4]Environnements et Paléoenvironnements Océaniques (EPOC), CNRS-UMR 5805, Université Bordeaux 1, Avenue des Facultés, 33405, Talence, France

[5] Institute of Biology, University of Southern Denmark, 5230 Odense, Denmark
[6] Faculty of Aquatic Sciences and Technology, University of Dar es Salaam, Tanzania

Received: 15 January 2007 – Accepted: 27 January 2007 – Published: 31 January 2007

Correspondence to: S. Bouillon (steven.bouillon@vub.ac.be)

## Abstract

We conducted diurnal sampling in a tidal creek (Ras Dege, Tanzania) to document the variations in a suite of creek water column characteristics and to determine the relative influence of tidal and biological driving forces. Since the creek has no upstream freshwater inputs, highest salinity was observed at low tide, due to evaporation effects and porewater seepage. Total suspended matter (TSM) and particulate organic carbon (POC) showed distinct maxima at periods of highest water flow, indicating that erosion of surface sediments and/or resuspension of bottom sediments were an important source of particulate material. Dissolved organic carbon (DOC), in contrast, followed the tidal variations and was highest at low tide. Stable isotope data of POC and DOC exhibit large variations in both pools, and followed tidal variations. Although the variation of $\delta^{13}C_{DOC}$ (−23.8 to −13.8‰) was higher than that of $\delta^{13}C_{POC}$ (−26.2 to −20.5‰) due to the different end-member pool sizes, the $\delta^{13}C$ signatures of both pools differed only slightly at low tide, but up to 9‰ at high tide. Thus, at low tide both DOC and POC originated from mangrove production. At high tide, on the other hand, the DOC pool had signatures consistent with a high contribution of seagrass-derived material, whereas the POC pool was dominated by marine phytoplankton. Daily variations in $CH_4$, and partial pressure of $CO_2$ ($pCO_2$) were similarly governed by tidal influence and were up to 7- and 10-fold higher at low tide, which stresses the importance of exchange of porewater and diffusive fluxes to the water column. Furthermore, this illustrates that constraining an ecosystem-level budget of these greenhouse gases in tidal systems requires a careful appraisal of tidal variations. When assuming that the high dissolved inorganic carbon (DIC) levels in the upper parts of the creek (i.e. at low tide) are due to inputs from mineralization, $\delta^{13}C$ data on DIC indicate that the source of the mineralized organic matter has a signature of −22.4‰, which shows that imported POC and DOC from the marine environment contributes strongly to overall mineralization within the mangrove system. Our data show a striking example of how biogeochemical processes in the intertidal zone appear to be prominent drivers of el-




BGD
4, 317–348, 2007

ement concentrations and isotope signatures in the water column, and how pathways of dissolved and particulate matter exchange are fundamentally different. The estimated export of DIC through porewater exchange appears considerably larger than for DOC, suggesting that if this mechanism is indeed a major driver of solute exchange, benthic mineralization and subsequent export as DIC could represent a very significant and previously unaccounted fate of mangrove-derived C. Budgeting efforts should therefore pay attention to understanding the mechanisms and quantification of different pathways of exchange within and between both zones.

## 1 Introduction

Vegetated coastal ecosystems are critical components of global ocean carbon and nutrient budgets. Despite their relatively small areal extent, their carbon sequestration represents a large inventory of organic matter; comparable to global riverine carbon discharges (e.g. see Ludwig et al., 1996; Gattuso et al., 1998). In addition to their carbon burial capacity (Duarte et al., 2005), these ecosystems are also "hotspots" in terms of mineralization (Middelburg et al., 2005) and $CO_2$ efflux to the atmosphere (e.g., Cai et al., 1999; Borges, 2005). Understanding the functioning of these diverse ecosystems and constraining their carbon and nutrient budgets is therefore of prime importance in improving the reliability of global oceanic budgets. The surface area of mangrove ecosystems worldwide declines by ~2% per year, implying major changes in the coastal carbon cycle (Duarte et al., 2005).

Mangrove ecosystems are limited to tropical and subtropical coastlines, but are known to be potentially significant sources of organic matter to adjacent estuaries and coastal waters on a global scale (Jennerjahn and Ittekkot, 2002; Dittmar et al., 2006). The biogeochemical functioning of mangrove environments is well constrained for a number of well-studied sites around the world, but our ability to elucidate carbon and nutrient budgets of these ecosystems and their impact on the coastal zone is still limited by basic gaps in our knowledge. The overall system productivity, for example, is

not well known since data on belowground allocation and wood productivity are scarce, but the few available data suggest that the overall C fixation is 3- to 4-fold higher than the typical values obtained from litterfall rate estimates (see Kristensen et al., 2007[1]). If this is indeed the case, previous budgets must be revised as other components in the overall budget are also significantly underestimated. Potentially important pathways in the carbon budget include burial into the sediment pool, export to coastal waters, and mineralization, but assessing their quantitative importance is not straightforward considering the variability observed within and among different mangrove systems due to e.g., differences in the geomorphology, hydrography, species composition, and tidal amplitude.

The exchange of material between the intertidal zone and the water column (estuary, lagoon, or tidal creeks) is a crucial aspect in understanding the functioning of these systems (Flindt et al., 2004, 2007). Previous work has demonstrated that particulate organic matter can be exported from mangrove systems, but at the same time suspended matter from the water column can be trapped and constitute an important source of organic matter to the intertidal zone (e.g., Hemminga et al., 1994; Bouillon et al., 2003, 2007). Exchange of dissolved organic matter and nutrients between intertidal areas and the water column can occur through (i) diffusive fluxes across the sediment/water interface during inundation, or (ii) porewater seepage into the water column during low and ebb tide. Fluxes across the sediment/water interface have been frequently studied, but typically show a large variability in the magnitude and direction of the fluxes for dissolved organic carbon (DOC) and inorganic N ($NH_4^+$ and $NO_3^-$) (e.g. Kristensen et al., 2000; Davis et al., 2001). The potential exchange of dissolved solutes through advective porewater seepage has been proposed previously (Ovalle et al., 1990; Dittmar and Lara, 2001; Borges et al., 2003; Barnes et al., 2006), but was found to be insignificant in other systems (Kristensen and Suraswadi, 2002). Such exchange mechanisms have also been proposed for salt marsh systems (Cai et al.,

[1]Kristensen, E., Bouillon, S., Dittmar, T., and Marchand, C.: Organic carbon dynamics in mangrove ecosystems, a review and speculative outlouk, Aquat. Bot., in review, 2007.

1999) and tidal freshwater marshes (Neubauer and Anderson, 2003; Gribsholt et al., 2005). The high metabolic activity in mangrove sediments create elevated porewater concentrations of total alkalinity (TA), dissolved inorganic carbon (DIC), DOC, and other metabolites (e.g., Marchand et al., 2006; Bouillon et al., 2007), and during ebb, porewaters can migrate into the water column and increase the concentrations of these solutes (Ovalle et al., 1990; Borges et al., 2003; Barnes et al., 2006). Porewater discharge into tidal creeks may also lower dissolved oxygen levels. The rate of porewater migration depends on the sediment permeability and the pressure gradient. Crab burrows have been found to dramatically enhance the hydraulic conductivity, and given their abundance in mangrove systems, these could be important mediators for subsurface flow of porewater to tidal creeks (Ridd, 1996; Susilo and Ridd, 2005; Mazda and Ikeda, 2006).

Recognizing and understanding the pathways of exchange between the intertidal zone and the adjacent water column is important for improving carbon budgets – this holds true not only for mangroves but also for other tidal systems such as salt marshes and tidal freshwater marshes. Mineralization rates measured in intertidal sediments (as $CO_2$ effluxes), for example, are likely to underestimate true mineralization rates if a significant part of the $CO_2$ (or DIC) generated is mobilized into the water column through seepage. Conversely, estimates of water-air $CO_2$ exchange in tidal creeks will overestimate creek water respiration if there is significant lateral input from porewater drainage. Lateral exchange of dissolved organic matter due to subsurface drainage from sediments and transfer to creeks represents a clear case of external subsidy for tidal creek organisms.

As part of a wider study comparing the carbon and nutrient dynamics of pristine and anthropogenically impacted mangrove systems in east Africa (PUMPSEA: "Peri-Urban Mangrove forests as filters and potential Phytoremediators of domestic Sewage in East Africa"), we investigated the tidal variations in water column biogeochemical signatures in a pristine mangrove creek along the Tanzanian coast, with a focus on the concentrations and origin of particulate organic carbon (POC), DOC, and DIC. This not

only provides a baseline study to compare with data from a nearby impacted mangrove system (which will be presented separately), but also fundamental data on the drivers for the often high variability in the water column biogeochemistry.

## 2 Materials and methods

Samples were collected on 16 and 17 September 2005 at hourly intervals during a diurnal cycle in a tidal creek at a location midway between its upper reaches and its opening towards the Indian Ocean in the Ras Dege mangrove forest, which is situated approximately 30 km southeast of Dar es Salaam, Tanzania (Fig. 1). The sampling period falls towards the end of the dry season. The mangrove forest in Ras Dege covers an area of 2.2 $km^2$, and is dominated by *Avicennia marina*, *Rhizophora mucronata*, *Sonneratia alba* and *Ceriops tagal*. The system comprises 2 tidal creeks which open into the Indian Ocean, and which receive no freshwater inputs except during the rainy season. The mouth of the creeks and the zone adjacent to the mouth is covered by seagrass beds.

Surface water for field measurements of dissolved $O_2$, pH, temperature and salinity were taken with a 1.7 L Niskin bottle ~0.5 m below the surface. Oxygen saturation level ($\%O_2$) was measured immediately after collection with a polarographic electrode (WTW Oxi-340) calibrated on saturated air, with an accuracy of ±1%. pH was measured using a Ross type combination electrode (ORION) calibrated on the NBS (US National Bureau of Standards) scale, as described by Frankignoulle and Borges (2001), with a reproducibility of ±0.005 pH units. Samples for determination of TA were obtained by pre-filtering 100 mL of water through precombusted Whatman GF/F filters followed by filtration through 0.2 $\mu$m cellulose acetate syringe filters (Sartorius), and were stored in HDPE bottles until analysis by automated electro-titration on 50 mL samples with 0.1 M HCl as titrant (reproducibility better than ±4 $\mu mol\,kg^{-1}$). The $pCO_2$ and DIC concentrations were computed from pH and TA measurements using the thermodynamic constants described in Frankignoulle and Borges (2001), with an accuracy of computed

DIC and $pCO_2$ values estimated at ±5 $\mu$mol kg$^{-1}$ and better than ±2%, respectively.

Water samples for the analysis of $\delta^{13}C_{DIC}$ were taken from the same Niskin bottle by gently overfilling 12 mL glass headspace vials, and poisoned with 20 $\mu$L of a saturated $HgCl_2$ solution. For the analysis of $\delta^{13}C_{DIC}$, a He headspace was created, and ~300 $\mu$L of $H_3PO_4$ was added to convert all inorganic carbon species to $CO_2$. After overnight equilibration, part of the headspace was injected into the He stream of an EA-IRMS (Elemental Analyzer – Isotope Ratio Mass Spectrometer; ThermoFinnigan Flash1112 and ThermoFinnigan Delta+XL) for $\delta^{13}C$ measurements. The obtained $\delta^{13}C$ data were corrected for the isotopic equilibration between gaseous and dissolved $CO_2$ using the algorithm presented in Miyajima et al. (1995). Water samples for the determination of $CH_4$ concentrations were taken directly from the Niskin bottle in 40 mL headspace vials, poisoned with $HgCl_2$, and capped with a butyl rubber plug and aluminium cap. $CH_4$ concentrations were determined by gas chromatography with flame ionization detection, after creating a headspace with $N_2$, as described in Abril and Iversen (2002). Certified $CH_4$:$N_2$ mixtures at 10 and 500 ppmv $CH_4$ were used as standards (Air Liquide, France). Dissolved $CH_4$ concentration was calculated with the solubility coefficient of Yamamoto et al. (1976). Reproducibility was generally better than 5%.

Samples for total suspended matter (TSM) were filtered immediately on pre-weighed and pre-combusted (overnight at 450°C) 47 mm Whatman GF/F filters, rinsed with mineral water to avoid salt contributions, and subsequently dried. Samples for particulate organic carbon (POC), particulate nitrogen (PN), and $\delta^{13}C_{POC}$ were filtered on pre-combusted 25 mm Whatman GF/F filters and dried. These filters were later decarbonated with HCl fumes under partial vacuum for 4 h, re-dried and packed in Ag cups. POC and PN were determined on a ThermoFinnigan Flash EA1112 using acetanilide as a standard, and the resulting $CO_2$ was measured on a ThermoFinnigan delta+XL interfaced via a Conflo III to the EA. Reproducibility of $\delta^{13}C_{POC}$ measurements was better than ±0.2‰. Samples for DOC and $\delta^{13}C_{DOC}$ were obtained by pre-filtering surface water on pre-combusted Whatman GF/F filters, followed by filtration on 0.2 $\mu$m cellulose

acetate syringe filters (Sartorius), and preserved by addition of 50 $\mu$L of $H_3PO_4$. DOC concentrations and $\delta^{13}C$ signatures were measured with a modified Thermo HiperTOC TOC-analyzer, interfaced with a Thermo delta +XL IRMS as described by Bouillon et al. (2006).

## 3 Results

The inner parts of the creek experienced a higher salinity than the outer part connected to the Indian Ocean, due to the absence of freshwater inputs and evaporation. This was reflected in the tidal variations in creek water with salinity values ranging from a high of almost 38 at low tide to less than 35 when oceanic water mixes in at high tide (Fig. 2).

TSM levels ranged between 60 and 95 mg $L^{-1}$ and showed two distinct tidal maxima (i.e. maxima occurred on three occasions, twice during ebb and once during flood), coinciding with periods of strong water currents (Fig. 3A). POC ranged between 0.31 and 4.06 mg C $L^{-1}$ and showed peak values at the same time as observed in TSM (Fig. 3B). These maxima also coincided with maxima in the contribution of POC to the TSM pool and with maxima in the POC/PN ratios (Figs. 3C, D). In contrast to POC, DOC showed variations that correlated strongly with salinity and mirrored those of the water column height, i.e. with lowest values at high tide and highest values at low tide (Fig. 4A). The stable isotope composition of both particulate and dissolved organic carbon showed strong tidal variations, both showing more depleted $\delta^{13}C$ signatures at low tide and enriched $\delta^{13}C$ values at high tide (Fig. 4B). However, variations in $\delta^{13}C_{POC}$ and $\delta^{13}C_{DOC}$ showed two important differences: (i) the fluctuations in $\delta^{13}C_{DOC}$ were delayed slightly relative to those of $\delta^{13}C_{POC}$, i.e. when the water level dropped, $\delta^{13}C$ signatures of the DOC pool responded later than those of the POC pool, and (ii) the amplitude of variation observed in $\delta^{13}C_{DOC}$ was more pronounced, ranging between −23.8 and −13.8‰, compared to a range between −26.2 and −20.5‰ for POC (Fig. 4B). These patterns, in combination with the different pool sizes, resulted in strong tidal difference

in $\delta^{13}C$ between both pools ($\Delta\delta$), showing minimum values of 0.3–2.5‰ at low tide and maximum values of 6.5–9.0‰ shortly after the peak of high tide (Fig. 4C).

Variations in $pCO_2$ and $CH_4$ concentrations were similar, being lowest at high tide and increasing drastically at low tide, reaching values 6- to 10-fold and 4- to 7-fold higher, respectively, than at high tide (Fig. 5A). The inorganic carbon pool showed similar dynamics as those in the DOC pool, i.e. highest TA and DIC at low tide (Fig. 5B). $\delta^{13}C$ signatures in the DIC pool were close to typical oceanic values (~0‰) at high tide, and became strongly negative during low tide, reaching ~−9‰ (Fig. 5C).

Oxygen saturation levels followed the tidal cycle and ranged from 59% at low tide to 111% at high tide (Fig. 5D). The level at high tide was dependent on light and exhibited higher values during daytime (100–110%) than during night (80–90%), likely due to oxygen production by primary producers during daytime.

## 4 Discussion

The Ras Dege mangrove forest showed characteristics of an 'inverse estuary', i.e. a tidal system without freshwater inputs where the salinity values are elevated at low tide in the upper reaches of the creek. This is a regular feature in mangrove creeks, and is typically observed during prolonged dry periods with high evaporation rates (Wolanski, 1986; Kitheka, 1996). Salinity variations therefore present a mirror image of the water column height (Fig. 2), showing typical oceanic values at high tide (~35), but increasing to nearly 38 at low tide. Porewater salinities at the forest floor (0–12 cm) measured during the same field campaign along the sampled creek showed high salinity levels, with an average of 39.5±2.2 (n=16) near the mouth of the creek and 47.4±4.7 (n=18) near the head of the creek. Assuming that porewater seepage is the main source of the elevated salinity at low tide, our data indicate that the porewater contribution to the creek at our sampling station is approximately 30% during the low tide slack, when water levels drop well below the creek bank level (Fig. 2, Table 1).

Export of particulate organic matter is considered an important feature of mangrove

systems and has been suggested to represent both a major fate of the ecosystem production and a significant source of organic matter to the adjacent marine environment (e.g. Lee, 1995; Jennerjahn and Ittekkot, 2002). Our tidal data show distinct peaks in the particulate matter pool and its composition when water current velocities are highest during each period of ebb and flood (Figs. 3A, B). Similar observations have been made in a degraded mangrove creek by Kitheka et al. (2002), who showed that TSM and POC maxima occurred at periods of highest current velocities in the front waters of the creek. The rapid increase in POC we observed coincides with an increase in POC/PN ratios (Fig. 3C), from values of ∼11–12 at high and low tide to >16 during tidal stage changes, indicating that there is a sudden coinciding change in the origin of the particulate organic matter pool. The high POC/PN ratios and depleted $\delta^{13}$C signatures (see Fig. 4B) both indicate that mangrove detritus is the main source of organic carbon during these events. Moreover, the peaks in the %POC/TSM during the current maxima (Fig. 3D) support the idea that the high levels of TSM and associated POC are caused by a rapid resuspension or mobilization of organic-rich surface sediments from the mangrove floor. Indeed, the upper 10 cm of intertidal sediments collected near to the sampling station contained TOC levels between 6.8 and 8.4%, TOC/TN ratios between 17.2 and 20.0, and $\delta^{13}$C values between −26.0 and −25.6‰.

Tidal variations of all dissolved constituents all followed a pattern that differs substantially from that of particulate matter. DOC concentrations closely followed the tidal changes in salinity, being highest at low tide (Fig. 4A), and were similar to the tidal variations observed by Dittmar and Lara (2001) in a Brazilian mangrove system and by Kristensen and Suraswadi (2002) in a Thai mangrove. These variations are consistent with average DOC concentrations of 7.4±2.6 mg C $L^{-1}$ (n=4) measured in sediment porewaters during the same field campaign. A simple mass balance calculation indicates that pore-water derived DOC contributes about 30% to the DOC pool during the low tide slack (Table 1). Similarly, oxygen in creek waters during low tide is strongly undersaturated because of a significant input of oxygen depleted pore-water. Assuming that no oxygen exchange occurred since pore-water drainage and until sampling at low

tide, we derive a pore-water contribution of 34% during the low tide slack, consistent with the estimates based on DOC and salinity (Table 1).

$\delta^{13}$C signatures of both DOC and POC varied substantially in phase with the tidal cycle, and showed a range of 10.0 and 5.7‰, respectively (Fig. 4B). Concentrations and $\delta^{13}$C values were clearly linked for each of these pools, and their co-variation is consistent with mixing between two pools of organic carbon, i.e. marine and mangrove end-members (Fig. 6). These relationships can thus be used to estimate the $\delta^{13}$C signature of the "added" DOC and POC from within the mangrove system. Mangrove end-member $\delta^{13}$C signatures based on the mixing curves are very similar: −26.6±0.3 and −26.7±0.3‰ for DOC and POC, respectively. These values are within the expected range for mangrove-derived organic carbon (Bouillon et al., 2007), confirming that mangrove primary production is the main source of organic matter derived from within the system boundaries. Moreover, this similarity indicates that despite potential differences in the biochemical composition of both pools, $\delta^{13}$C signatures of both POC and DOC derived from mangrove litter are similar. The latter is an important prerequisite to use these tracers in distinguishing the contribution of different sources to the POC and DOC pools and to unambiguously interpret small but significant differences in the $\delta^{13}$C composition of both pools as a difference in their source contributions (e.g. see Bouillon et al., 2007). However, marine end-member $\delta^{13}$C signatures for DOC and POC differ substantially, and demonstrate a distinct difference in their origin. Whereas the POC pool shows signatures typical for marine phytoplankton (-20 to −22‰, e.g. Fontugne and Duplessy, 1981), the DOC pool is much more $^{13}$C-enriched with $\delta^{13}$C values around −16 to −14‰. This is much more enriched than can be expected for marine phytoplankton, but seagrasses found at the creek mouths and which cover large areas on the slope outside the system are expected to have $\delta^{13}$C values within this range. Although $\delta^{13}$C signatures for seagrasses were not determined in this particular system, other data from the east African coast range between −18.6 and −10.7‰ (Bouillon et al., 2004; Macia, 2004). This difference in end-member $\delta^{13}$C signatures and in the timing of local maxima during the tidal cycle results in an offset in $\delta^{13}$C sig-



BGD
4, 317–348, 2007



EGU

natures between the dissolved and particulate pools. Thus, $\Delta\delta$ (defined as $\delta^{13}C_{DOC}$ – $\delta^{13}C_{POC}$) is minimal (0–2‰) at low tide, whereas large differences of up to 9‰ are observed during or shortly after high tide (Fig. 4C). Differences in the origin of particulate and dissolved organic carbon have previously been documented (Bouillon et al., 2006), but rarely as pronounced as shown here. More importantly, our study provides a clear mechanism for these strong variations.

Mangroves and salt marshes have been considered as systems where a significant part of the ecosystem production is exported to the adjacent coastal zone (the "outwelling" hypothesis), and it has been suggested that most of the organic carbon is exported in the dissolved form (e.g., Lee, 1995; Dittmar et al., 2006). DOC was indeed found to be the dominant organic C pool in the water column, comprising ~70% of the total water column organic carbon pool during low tide. Moreover, our study revealed that a major part originated from pore-water drainage and coupling data such as those collected here with hydrodynamic modelling should provide a better understanding of the import/export of organic matter in these tidal systems and the relative importance of particulate and dissolved export (Flindt et al., unpublished data). Import of organic matter of marine origin has recently gained attention, since the water column can provide an important source of organic matter to intertidal sediments and thereby to microbial and invertebrate communities in the intertidal zone (Bouillon et al., 2007[2]).

TA, DIC, and $pCO_2$ showed tidal variations similar to those of DOC, i.e. their concentrations were inversely related to the tidal height (Figs. 5A, B), consistent with results from previous studies (e.g. Borges et al., 2003). The observed range in $pCO_2$ is extremely high (Figure 5A), with low tide levels up to 10-fold those at high tide and corresponding to an amplitude of ~4500 ppm, similar to the one of ~3500 ppm reported by Borges et al. (2003) during a diurnal cycle in an Indian mangrove creek. The emission of $CO_2$ to the atmosphere computed with the Raymond and Cole (2001)

[2]Bouillon, S., Connolly, R., and Lee, S. Y.: Carbon exchange and cycling in mangrove ecosystems: a synthesis of recent insights based on stable isotope studies, J. Sea Res., in review, 2007.

gas transfer velocity parameterisation (using wind speed data measured with a hand-held anemometer) was on average 33 mmol $m^{-2}$ $d^{-1}$ (range 1–80 mmol $m^{-2}$ $d^{-1}$). Such high $CO_2$ emission rates are consistent with estimates previous studies which range between ~1 and ~200 mmol $m^{-2}$ $d^{-1}$ and show an average of ~50 mmol $m^{-2}$ $d^{-1}$ for different sites (Borges et al., 2003).

The inorganic carbon data presented here are again consistent with a strong influence of porewaters, which typically show high TA, high DIC and $pCO_2$ (e.g. Bouillon et al., 2007; simultaneously measured porewater DIC along the Ras Dege creek ranged up to 6 mM). As has been previously stressed for salt marshes and tidal freshwater marshes (Cai et al., 1999; Neubauer and Anderson, 2003), high $pCO_2$ values in the water column do not necessarily imply a net heterotrophic water column, but can to some extent also be caused by mineralization in the intertidal areas and subsequent transport to the creek. Such an exchange mechanism thus acts as a $CO_2$ "pump", transporting $CO_2$ generated in intertidal sediments towards the water column where $CO_2$ efflux towards the atmosphere takes place. The only evidence of photosynthetic production in the water column at Ras Dege was the occurrence of distinctly higher oxygen saturation at high tide during the day than during the night (Fig. 5D). The $\delta^{13}C_{DIC}$ (range between −9.4 and +0.5‰) closely followed the tidal height (Fig. 5C), and was inversely related to DIC concentrations (Fig. 7). The resulting inverse first order polynomial relationship between these variables is consistent with simple conservative mixing between two carbon sources. Assuming that the build-up of DIC is essentially due to mineralization, and neglecting the effect of $CO_2$ outgassing on $\delta^{13}C$ signatures of the DIC pool (which is acceptable as shown by the conservative fit in Fig. 7), the $\delta^{13}C$ signature of the "added" DIC can be estimated to −22.4±0.4‰ from the relationship between DIC and $\delta^{13}C_{DIC}$. $Ca^{2+}$ data (not shown) do not indicate noticeable calcium carbonate dissolution, which further indicates that this approach is valid in our system. The estimated $\delta^{13}C$ signal for the DIC produced is higher than expected if mangrove biomass (~−27‰) or bulk sediment organic matter (~−25‰) were the only organic matter sources for mineralization, but is close to the average signatures of

the total (DOC and POC) water column organic carbon pool during one full tidal cycle (−21.9±3.2‰). Thus, our data suggest that both marine organic matter (phytoplankton and seagrass-derived) and mangrove detritus contribute to mineralization within the mangrove forest boundary. This had been demonstrated previously based on isotope data of bacterial markers (e.g. Bouillon et al., 2004), yet such data only referred to the upper layers of the sediments, where inputs of non-mangrove sources are likely to be most important (i.e. microbenthic production and deposition of suspended matter from the water column). Since mineralization in deeper sediment layers – where the organic matter is often to a larger extent mangrove-derived, e.g. Marchand et al. (2003) – can also reach high levels (Alongi et al., 2004), previous evidence from bacterial markers did not necessarily demonstrate the importance of allochtonous (i.e. non-mangrove) sources at the entire ecosystem level, whereas the approach used here does confirm that marine-derived organic matter contributes substantially to the integrated mineralization within the mangrove system boundaries.

The daily variations of $CH_4$ in Ras Dege creek waters are similar to those recently reported for a mangrove creek on South Andaman Island (Barnes et al., 2006), except that the concentration range is lower in Ras Dege (13–142 nmol $L^{-1}$) than observed by Barnes et al. (2006; range 282–704 nmol $L^{-1}$). In the Sundarban mangrove forest fringe (Hooghly estuary), Biswas et al. (2007) reported a similar $CH_4$ concentration range (range 11–130 nmol $L^{-1}$) as in this study, with variations roughly in phase with those of salinity (3–26). They observed that daily variations of $CH_4$ were driven by the mixing of freshwaters (with lower $CH_4$ concentrations) with seawater draining the mangrove forests (with higher $CH_4$ concentrations). Both variables were dominated by the advection of water masses with different chemical signatures, since their station was located at the fringe of the mangrove (i.e. a low influence of intertidal zones) and because the salinity variations were largely dominated by estuarine mixing, due to the influence of freshwater inputs from the Hoogly River. This is consistent with much larger signals in the salinity amplitude and lower signal in the $CH_4$ amplitude than in Ras Dege (this study) and South Andaman Island creeks (Barnes et al., 2006). The average

emission of $CH_4$ to the atmosphere during the tidal cycle (computed with the Raymond and Cole (2001) gas transfer velocity parameterisation) was 29 $\mu$mol m$^{-2}$ d$^{-1}$, ranging between 0 and 185 $\mu$mol m$^{-2}$ d$^{-1}$, similar to those reported by Biswas et al. (2007) (2–135 $\mu$mol m$^{-2}$ d$^{-1}$) but lower than the fluxes observed by Barnes et al. (2006) (432–840 $\mu$mol m$^{-2}$ d$^{-1}$). It should be noted that $CH_4$ emission from mangrove waters to the atmosphere can be several orders of magnitude lower than from the sediments ranging between −19 and 19 500 $\mu$mol m$^{-2}$ d$^{-1}$ (compiled in Barnes et al., 2006). Furthermore, the computed diffusive $CH_4$ fluxes under-estimate the overall $CH_4$ emission due to a large but highly variable contribution of ebullition $CH_4$ fluxes (Barnes et al., 2006).

Nevertheless, $CH_4$ emission from mangrove systems are low when compared to freshwater wetland systems (Bartlett and Harriss, 1983), except in anthropogenically disturbed mangrove systems (Purvaja and Ramesh, 2001; Sotomayor et al., 1994; Giani et al., 1996; Alongi et al., 2005). This can be ascribed to different reasons: first, methanogenesis in mangrove sediments typically represents less than 2% of the overall C degradation, which is generally dominated by sulphate reduction and/or Fe reduction (Alongi, 1998); secondly, the presence of sulphates can favour anaerobic oxidation of $CH_4$ (Giani et al., 1996; Biswas et al., 2007), and finally, the dominance of clay minerals and the frequent mobilization of surface sediments by tidal currents in mangroves systems can enhance aerobic methane oxidation both at the sediment surface and in the water column (Weaver and Dugan, 1972; Abril et al., 2007).

In summary, the observed daily variations in water column chemistry and isotopic signatures can be explained by different exchange processes for dissolved and particulate matter pools, as conceptualized in Fig. 8. There are two main sources of dissolved constituents, i.e. porewater seepage and marine inputs, and two main sources of particulate material, i.e. sediment detritus and marine particulate organic matter. The origin of both particulate and dissolved organic matter from within the system appears to be predominantly mangrove-derived based on the $\delta^{13}C$ signatures (Fig. 6). In contrast, while the marine source of DOC appears to be to a large extent derived from $^{13}C$-enriched seagrass material, marine POC seems predominantly of phytoplankton

origin (Fig. 6). The carbon transport during high tide is dominated by diffusive solute (DOC, DIC) fluxes across the sediment-water interface (period A in Fig. 8), and settling of POC from the water column which to some extent is of marine phytoplankton origin (not shown in Fig. 8). During ebb (period B in Fig. 8), there is porewater solute seepage resulting in increasing concentrations of gradually more $^{13}$C-depleted DOC and DIC in the creek water, as well as higher $CH_4$ and $pCO_2$ values and lower $O_2$ saturation levels. During tidal transitions, there is mobilization of particulate material likely through resuspension and sediment erosion, which causes a rapid increase in mangrove-derived TSM and POC as indicated by a decrease in $\delta^{13}C_{POC}$ and an increase in POC/PN ratios and %POC/TSM in the creek water. As the water current decreases towards low tide slack (period C in Fig. 8), the particulate material (TSM and POC) settles down again, but $\delta^{13}C_{POC}$ signatures remain low reflecting the dominance of mangrove-derived material. When the flood starts (period D in Fig. 8), the concentration of particulate material dominated by oceanic water signatures transiently increases with maximal tidal currents and then decreases until high tide slack.

Biogeochemical processes in the intertidal zone, erosion of surface sediments, and exchange of porewater combined with the physical conditions related to the tidal cycle are thus important drivers of the concentrations and isotopic signatures of dissolved and particulate carbon in mangrove creek waters. Other processes responsible for enhanced exchange of particulate matter between intertidal zones and creek waters such as precipitation (Barnes et al., 2006) were not captured in the present dataset. Also, the exchange of solutes in mangrove environments is likely enhanced by burrow structures constructed by the resident fauna. Crab burrows, which are often very densely distributed, have been demonstrated to increase the hydraulic conductivity of mangrove sediments (Ridd, 1996; Susilo and Ridd, 2005; Susilo et al., 2005) and create a larger effective surface area where diffusive exchange of solutes between the sediment and water can take place. Their role in enhancing direct solute exchange can thus be considered as an additional aspect of their importance as "ecosystem

engineers" (Kristensen, 2007[3]) in mangrove systems.

Global mangrove C budgets are still poorly constrained and when realizing that litterfall likely constitutes only ~30% of the total mangrove $CO_2$ fixation (e.g. Alongi et al., 2005), a major part of the systems' production (i.e. including belowground production) cannot be accounted for with the currently available data (see Kristensen et al., 2007[1]). Considering that mineralization rates are typically derived from core incubations where the exchange of $CO_2$ across the sediment/air or sediment/water interface is taken as a proxy for total sediment mineralization, it would appear plausible that the observed build-up of DIC in sediment porewaters due to mineralization and its subsequent exchange with the water column represents at least one of the "missing links" in providing more robust carbon budgets for these ecosystems. In this particular system, the difference between low-tide and high-tide concentrations of DIC were approximately 7 times as large as the observed difference for DOC (~13 mg C $L^{-1}$ for DIC vs ~1.8 mg C $L^{-1}$ for DOC), suggesting that if porewater exchange is a major driver of carbon exchange, benthic mineralization and subsequent export as DIC could represent a very significant and previously unaccounted flux of mangrove-derived C.

*Acknowledgements.* S. B. is funded by a postdoctoral mandate from the Research Foundation Flanders (FWO-Vlaanderen), and was partly accomplished during a postdoctoral stay at the NIOO-CEME. A. V. B. is a research associate with the FNRS, Belgium. This research was funded by the EC-STREP programme PUMSPEA (contract 510863), and the $\delta^{13}$C-DOC analyses were made possible through a research grant from the FWO-Vlaanderen (contract 1.5.070.05) and the Research Council of the Vrije Universititeit Brussel. Thanks are due to Y. P. Mhonda for his cheerful company during the 24-h sampling, to M. Korntheuer for his excellent technical help in setting up and maintaining the DOC-IRMS, and to G. Neukermans for providing details on the mangrove vegetation and extent in the study area. D. P. Gillikin provided useful comments to this manuscript.

[3]Kristensen, E.: Mangrove crabs as ecosystem engineers, with emphasis on sediment processes, J. Sea Res., in review, 2007.

## References


Abril, G. and Iversen, N.: Methane dynamics in a shallow, non-tidal, estuary (Randers Fjord, Denmark), Mar. Ecol. Prog. Ser., 230, 171–181, 2002.

Abril, G., Commarieu, M.-V., and Guérin, F., : Enhanced methane oxidation in an estuarine turbidity maximum, Limnol. Oceanogr., 52, 470–475, 2007.

Alongi, D. M.: Coastal ecosystem processes, CRC Press, 419 p., 1998.

Alongi, D. M.: Present state and future of the world's mangrove forests, Environ. Conserv., 29, 331–349, 2005.

Alongi, D. M., Sasekumar, A., Chong, V. C., Pfitzner, J., Trott, L. A., Tirendi, F., Dixon, P., and Brunskill, G. J.: Sediment accumulation and organic material flux in a managed mangrove ecosystem: estimates of land-ocean-atmosphere exchange in peninsular Malaysia, Mar. Geol., 208, 383–402, 2004.

Alongi, D. M., Clough, B. F., and Robertson, A. I.: Nutrient-use efficiency in arid-zone forests of the mangroves *Rhizophora stylosa* and *Avicennia marina*, Aquat. Bot., 82, 121–131, 2005.

Alongi, D. M., Pfitzner, J., Trott, L. A., Dixon, P., and Klumpp, D. W.: Rapid sediment accumulation and microbial mineralization in forests of the mangrove *Kandelia candel* in the Jiulongjiang estuary, China, Estuar. Coast. Shelf Sci., 63, 605–618, 2005.

Bartlett, K. B. and Harriss, R. C.: Review and assessment of methane emissions from wetlands, Chemosphere, 26, 261–320, 1993.

Barnes, J., Ramesh, R., Purvaja, R., Nirmal Rajkumar, A., Senthil Kumar, B., Krithika, K., Ravichandran, K., Uher, G., and Upstill-Goddard, R.: Tidal dynamics and rainfall control $N_2O$ and $CH_4$ emmissions from a pristine mangrove creek, Geophys. Res. Lett., 33, L15405, doi:10.1029/2006GL026829, 2006.

Biswas, H., Mukhopadhyay, S. K., Sen, S., and Jana, T. K.: Spatial and temporal patterns of methane dynamics in the tropical mangrove dominated estuary, NE coast of Bay of Bengal, India, J. Mar. Syst., doi:10.1016/j.jmarsys.2006.11.001, 2007.

Borges, A. V.: Do we have enough pieces of the jigsaw to integrate $CO_2$ fluxes in the Coastal Ocean?, Estuaries, 28, 3–27, 2005.

Borges, A. V., Djenidi, S., Lacroix, G., Théate, J., Delille, B., and Frankignoulle, M.: Atmospheric $CO_2$ flux from mangrove surrounding waters, Geophys. Res. Lett., 30, 1558, doi: 10.1029/2003GL017143, 2003.

Bouillon, S., Frankignoulle, M., Dehairs, F., Velimirov, B., Eiler, A., Etcheber, H., Abril, G., and

Borges, A. V.: Inorganic and organic carbon biogeochemistry in the Gautami Godavari estuary (Andhra Pradesh, India) during pre-monsoon: the local impact of extensive mangrove forests, Glob. Biogeochem. Cycles, 17, 1114, doi:10.1029/2002GB002026, 2003.

Bouillon, S., Moens, T., and Dehairs, F.: Carbon sources sustaining benthic mineralization in mangrove and adjacent seagrass sediments (Gazi bay, Kenya), Biogeosciences, 1, 71–78, 2004, http://www.biogeosciences.net/1/71/2004/.

Bouillon, S., Korntheuer, M., Baeyens, W., and Dehairs, F.: A new automated setup for stable isotope analysis of dissolved organic carbon, Limnol. Oceanogr.: Methods, 4, 216–226, 2006.

Bouillon, S., Dehairs, F., Schiettecatte, L.-S., and Borges, A. V.: Biogeochemistry of the Tana estuary and delta (northern Kenya), Limnol. Oceanogr., 52, 46–59, 2007.

Cai, W.-J., Pomeroy, L. R., Moran, M. A., and Wang, Y.: Oxygen and carbon dioxide mass balance for the estuarine-intertidal marsh complex of five rivers in the southeastern U.S., Limnol. Oceanogr., 44, 639–649, 1999.

Cai, W.-J., Wiebe, W. J., Wang, Y., and Sheldon, J. E.: Intertidal marsh as a source of dissolved inorganic carbon and a sink of nitrate in the satilla river-estuarine complex in the southeastern U.S. Limnol. Oceanogr., 45, 1743–1752, 2000.

Davis, S. E., Childers, D. L., Day, J. W., Rudnick, D. T., and Sklar, F. H.: Wetland-water column exchanges of carbon, nitrogen, and phosphorus in a southern Everglades dwarf mangrove, Estuaries, 24, 610–622, 2001.

Dittmar, T. and Lara, R. J.: Driving forces behind nutrient and organic matter dynamics in a mangrove tidal creek in North Brazil, Estuar. Coast. Shelf Sci., 52, 249–259, 2001.

Dittmar, T., Hertkorn, N., Kattner, G., and Lara, R. J.: Mangroves, a major source of dissolved organic carbon to the oceans, Glob. Biogeochem. Cycles, 20, GB1012, doi: 10.1029/2005GB002570, 2006.

Duarte, C. M., Middelburg, J. J., and Caraco, N.: Major role of marine vegetation on the oceanic carbon cycle, Biogeosciences, 2, 1–8, 2005, http://www.biogeosciences.net/2/1/2005/.

Flindt, M. R., Neto, J., Amos, C. L., Pardal, M. A., Bergamasco, A., Pedersen, C. B., and Andersen, F. Ø.: Plant bound nutrient transport. Mass transport in estuaries and lagoons, in: Estuarine nutrient cycling: the influence of primary producers. The fate of nutrient biomass, edited by: Nielsen, S. L., Banta, G. T., and Pedersern, M. F., Series: Aquatic Ecology, Vol. 2,

93–128, 2004.
Flindt, M. R., Pedersen, C. B., Amos, C. L., Levy, A., Bergamasco, A., and Friend, P. L.: Transport, sloughing and settling rates of estuarine macrophytes: mechanisms and ecological implications, Cont. Shelf Res., in press, 2007.
Fontugne, M. R. and Duplessy, J. C.: Organic carbon isotopic fractionation by marine plankton in the temperature range −1 to 31°C, Oceanol. Acta, 4, 85–90, 1981.
Frankignoulle, M. and Borges, A. V.: Direct and indirect $pCO_2$ measurements in a wide range of $pCO_2$ and salinity values (the Scheldt estuary), Aquat. Geochem., 7, 267–273, 2001.
Gattuso, J.-P., Frankignoulle, M., and Wollast, R.: Carbon and carbonate metabolism in coastal aquatic ecosystems, Ann. Rev. Ecol. Syst., 29, 405–433, 1998.
Giani, L., Bashan, Y., Holguin, G., and Strangmann, A.: Characteristics and methanogenesis of the Balandra lagoon mangrove soils, Baja California Sur, Mexico, Geoderma, 72, 149–160, 1996.
Gribsholt, B., Boschker, H. T. S., Struyf, E., Andersson, M., Tramper, A., De Brabandere, L., Van Damme, S., Brion, N., Meire, P., Dehairs, F., Middelburg, J. J., and Heip, C.: Nitrogen processing in a tidal freshwater marsh: a whole ecosystem $^{15}N$ labeling study, Limnol. Oceanogr., 50, 1945–1959, 2005.
Jennerjahn, T. C. and Ittekkot, V.: Relevance of mangroves for the production and deposition of organic matter along tropical continental margins, Naturwissenschaften, 89, 23–30, 2002.
Kitheka, J. U.: Water circulation and coastal trapping of brackish water in a tropical mangrove-dominated bay in Kenya, Limnol. Oceanogr., 41, 169–176, 1996.
Kitheka, J. U., Ongwenyi, G. S., and Mavuti, K. M.: Dynamics of suspended sediment exchange and transport in a degraded mangrove creek in Kenya, Ambio, 31, 580–587, 2002.
Kristensen, E., Andersen, F. O., Holmboe, N., Holmer, M., and Thongtham, N.: Carbon and nitrogen mineralization in sediments of the Bangrong mangrove area, Phuket, Thailand, Aquat. Microb. Ecol., 22, 199–213, 2000.
Kristensen, E. and Suraswadi, P.: Carbon, nitrogen and phosphorus dynamics in creek water of a southeast Asian mangrove forest, Hydrobiologia, 474, 197–211, 2002.
Lee, S. Y.: Mangrove outwelling: a review, Hydrobiologia, 295, 203–212, 1995.
Macia, A.: Primary carbon sources for juvenile penaeid shrimps in a mangrove-fringed Bay of Inhaca Island, Mozambique: a dual carbon and nitrogen isotope analysis, W. Ind. Ocean J. Mar. Sci., 3, 151—161, 1995.
Marchand, C., Lallier-Vergès, E., and Baltzer, F.: The composition of sedimentary organic

matter in relation to the dynamic features of a mangrove-fringed coast in French Guiana, Estuar. Coast. Shelf Sci., 56, 119–130, 2003.
Marchand, C., Albéric, P., Lallier-Vergès, E., and Baltzer, F.: Distribution and characteristics of dissolved organic matter in mangrove sediment pore waters along the coastline of French Guiana, Biogeochem., 81, 59–75, 2006.
Mazda, Y. and Ikeda, Y.: Behavior of the groundwater in a riverine-type mangrove forest, Wetl. Ecol. Manag., 14, 477–488, 2006.
Middelburg, J. J., Duarte, C. M., and Gattuso, J.-P.: Respiration in coastal benthic communities, in: Respiration in aquatic ecosystems, edited by: del Giorgio, P. A. and Williams, P. J. le B., Oxford Univ. Press, 2005.
Miyajima, T., Yamada, Y., Hanba, Y. T., Yoshii, K., Koitabashi, T., and Wada, E.: Determining the stable-isotope ratio of total dissolved inorganic carbon in lake water by GC/C/IRMS, Limnol. Oceanogr., 40, 994–1000, 1995.
Ovalle, A. R. C, Rezende, C. E., Lacerda, L. D., and Silva, C. A. R.: Factors affecting the hydrochemistry of a mangrove tidal creek, Sepetiba Bay, Brazil, Estuar. Coast. Shelf Sci., 31, 639–650, 1990.
Purvaja, R. and Ramesh, R.: Natural and anthropogenic methane emission from wetlands of south India, Environ. Manag., 27, 547–557, 2001.
Purvaja, R., Ramesh, R., and Frenzel, P.: Plant-mediated methane emission from an Indian mangrove, Glob. Change Biol., 10, 1825–1834, 2004.
Raymond, P. A. and Cole, J. J.: Gas exchange in rivers and estuaries: choosing a gas transfer velocity, Estuaries, 24, 312–317, 2001.
Ridd, P. V.: Flow through animal burrows in mangrove creeks, Estuar. Coast. Shelf Sci., 43, 617–625, 1996.
Sotomayor, D., Corredor, J. E., and Morell, J. M.: Methane flux from mangrove sediments along the Southwestern Coast of Puerto Rico, Estuaries, 17, 140–147, 1994.
Susilo, A. and Ridd, P. V.: The bulk hydraulic conductivity of mangrove soil perforated with animal burrows, Wetl. Ecol. Manag., 13, 123–133, 2005.
Susilo, A., Ridd, P. V., and Thomas, S.: Comparison between tidally driven groundwater flow and flushing of animal burrows in tropical mangrove swamps, Wetl. Ecol. Manag., 13, 377–388, 2005.
Victor, S., Golbuu, Y., Wolanski, E., and Richmond, R. H.: Fine sediment trapping in two mangrove-fringed estuaries exposed to contrasting land-use intensity, Palau, Micronesia,

Wetl. Ecol. Manag., 12, 277–283, 2004.
Weaver, T. L. and Dugan, P. R.: Enhancement of bacterial methane oxidation by clay minerals, Nature, 237, 518, 1972.
Wolanski, E.: An evaporation-driven salinity maximum in Australian tropical estuaries, Estuar. Coast. Shelf Sci., 22, 415–424, 1986.
Yamamoto, S., Alcauskas, J. B., and Crozier, T. E.: Solubility of methane in distilled water and seawater, J. Chem. Eng. Data., 21, 78–80, 1976.

**Table 1.** Estimated porewater contributions to the creek water column at low tide, based on salinity, DOC, and $\%O_2$ data on porewaters and in creek waters during high tide and low tide, and (lower part) calculated porewater $CH_4$, TA and DIC based on an average estimated porewater contribution of 31%. Porewaters were assumed to be anoxic (i.e. $\%O_2$=0), porewater salinity data and DOC concentrations: E. Kristensen, unpublished data.

| | Porewater | Ebb | Flood | % porewater during ebb |
|---|---|---|---|---|
| Salinity | 43.5 (average) | 37.5 | 34.8 | **31%** |
| | 49.1 (high) | 37.5 | 34.8 | **19 %** |
| | 37.9 (low) | 37.5 | 34.8 | **87 %** |
| DOC ($mg\,C\,L^{-1}$) | 7.40 (avg) | 2.57 | 0.79 | **27 %** |
| | 9.99 (high) | 2.57 | 0.79 | **19 %** |
| | 4.81 (low) | 2.57 | 0.79 | **44 %** |
| $\%O_2$ | 0 | 59 | 91 | **34 %** |

Estimated porewater concentrations using a fixed average porewater contribution:

| | Ebb | Flood | % porewater | Estimated porewater concentration |
|---|---|---|---|---|
| $CH_4$ (nM) | 112 | 19 | 31% | **319** |
| TA ($mmol\,kg^{-1}$) | 3.36 | 1.97 | 31% | **6.46** |
| DIC ($mmol\,kg^{-1}$) | 3.34 | 2.29 | 31% | **5.66** |

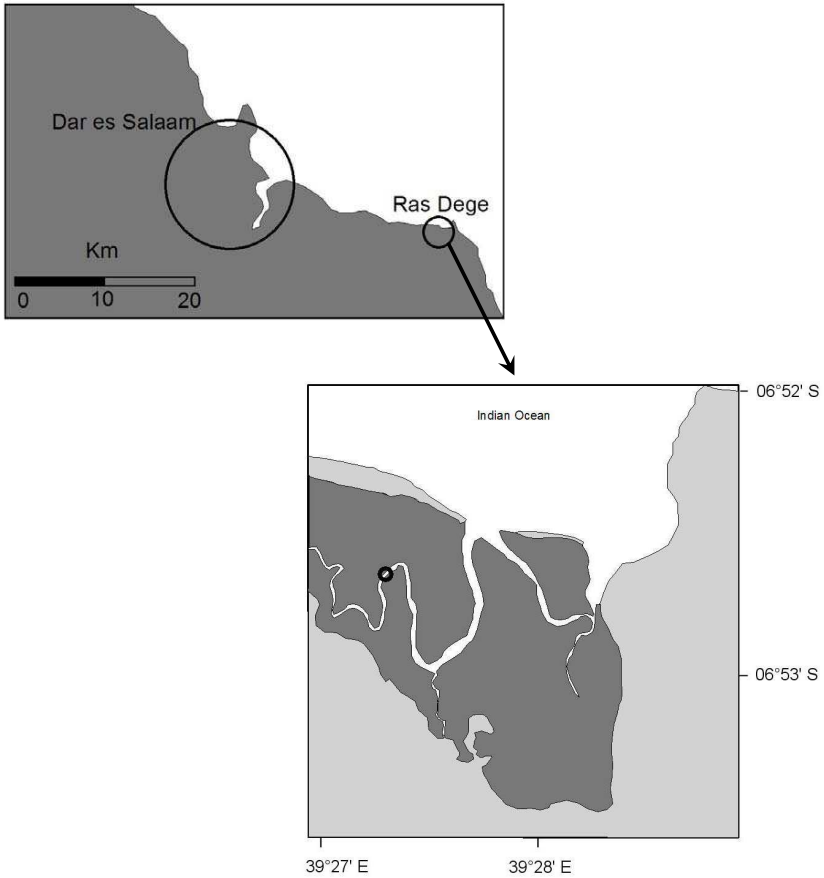


**Fig. 1.** Location of the study area and the sampling site. Darkest areas indicate the areal cover of mangrove vegetation.



BGD
4, 317–348, 2007



EGU

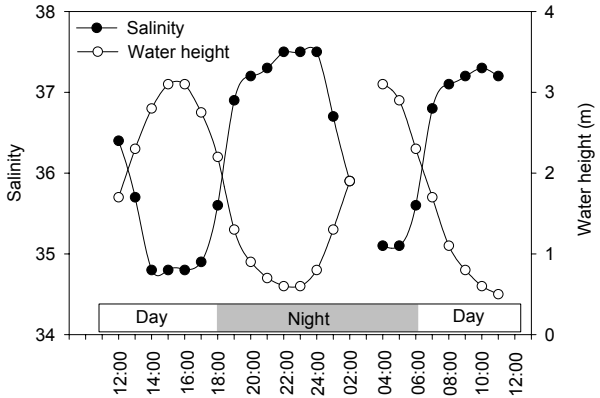


**Fig. 2.** Tidal variations of salinity in surface waters and water height.

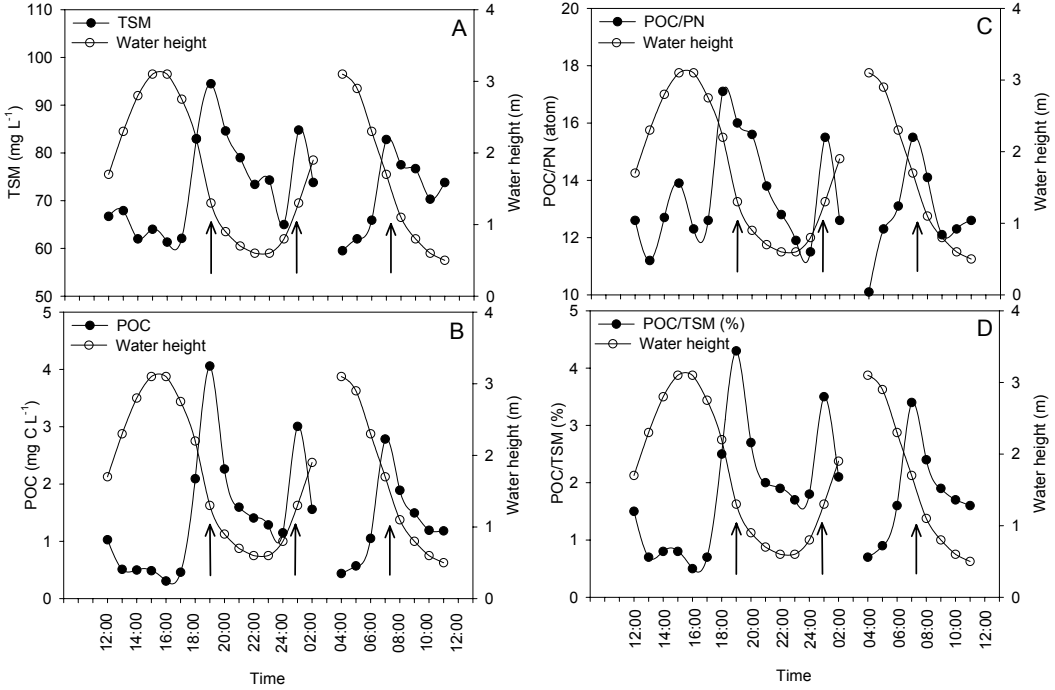


**Fig. 3.** Tidal variations of water height and **(A)** total suspended matter, **(B)** particulate organic carbon, **(C)** POC/PN ratios (atom) of suspended matter, and **(D)** the % contribution of POC to the TSM pool. Arrows indicate distinct maxima coinciding with highest tidal currents.

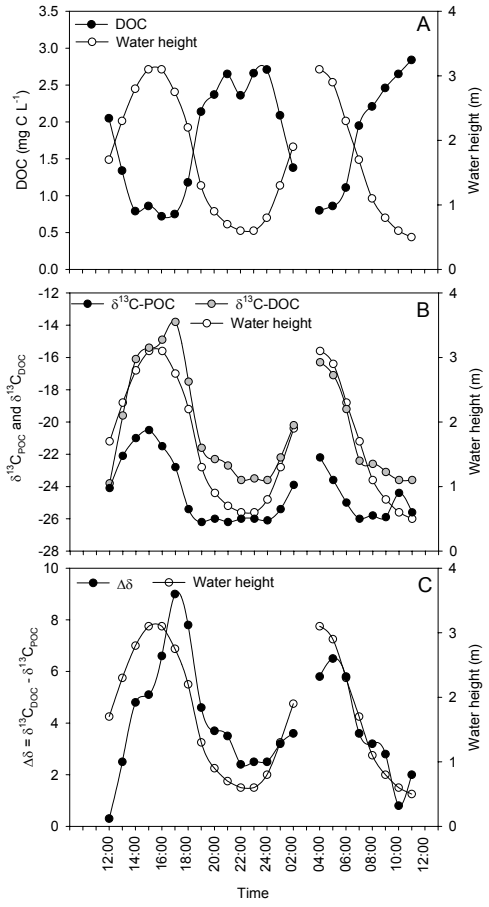


**Fig. 4.** Tidal variations of water height and **(A)** dissolved organic carbon concentrations, **(B)** carbon stable isotope signatures in particulate and dissolved organic carbon, and **(C)** the difference in $\delta^{13}$C between DOC and POC.

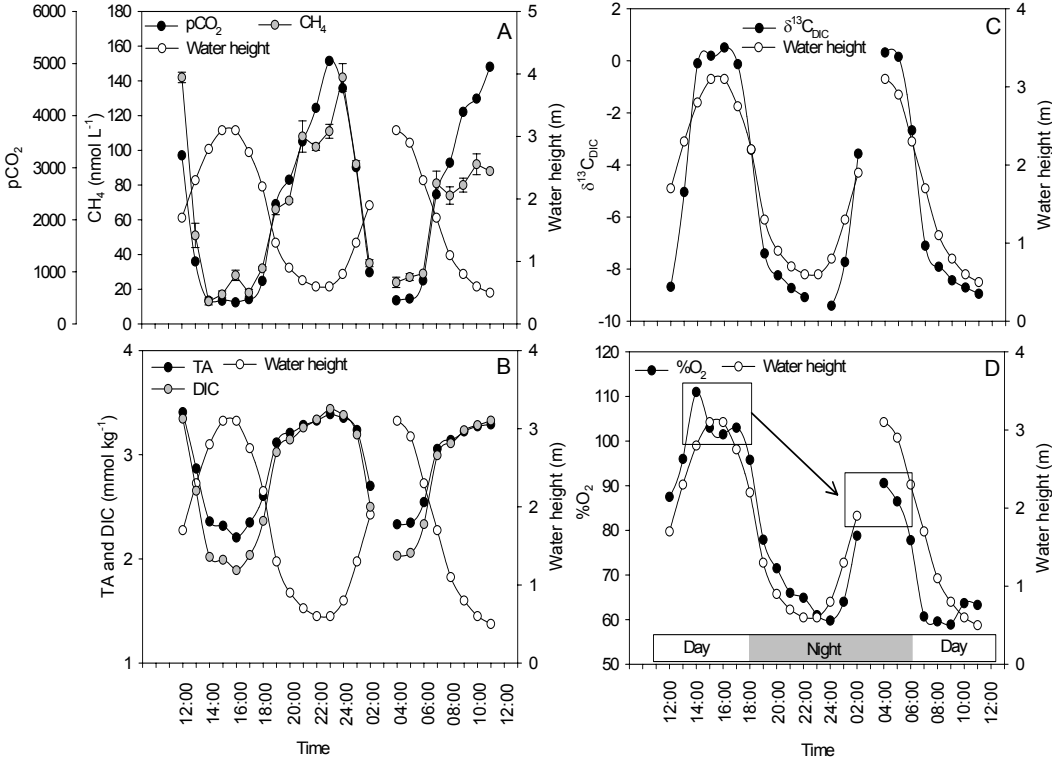


**Fig. 5.** Tidal variations of water height and **(A)** $CH_4$ concentrations and $pCO_2$, **(B)** total alkalinity and dissolved inorganic carbon concentrations, **(C)** $\delta^{13}C$ signatures of dissolved inorganic carbon, and **(D)** dissolved oxygen saturation levels ($\%O_2$). Error bars on the $CH_4$ concentrations are 1 s.d., based on triplicate measurements.



BGD
4, 317–348, 2007

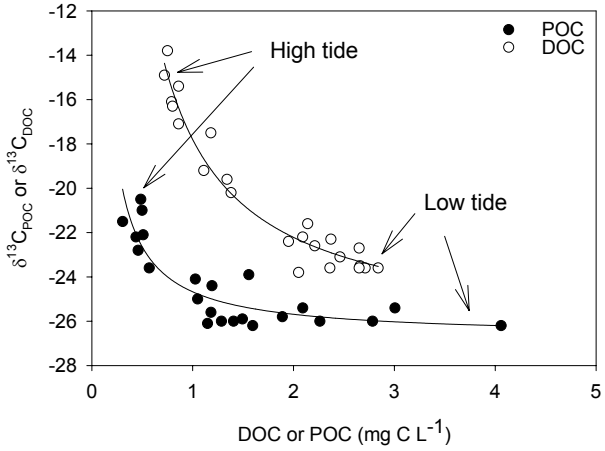


**Fig. 6.** Concentrations and $\delta^{13}$C signatures of particulate and dissolved organic carbon (dark and open symbols, respectively) during a diurnal cycle. Lines represent a fitted inverse first order polynomial, of the form $y=y_0+a/x$, with $y_0=-26.6\pm0.3$ for DOC and $-26.7\pm0.3$ (1 S.E.) for POC (see text for details).

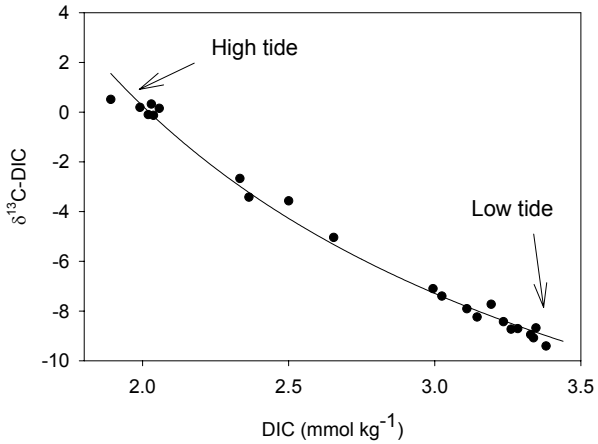


**Fig. 7.** Correlation between dissolved inorganic carbon concentrations and its stable isotope composition for samples collected during a diurnal cycle. Full line represents a fitted first order polynomial, of the form $y=y_0+a/x$, with $y_0=-22.4\pm0.4$.

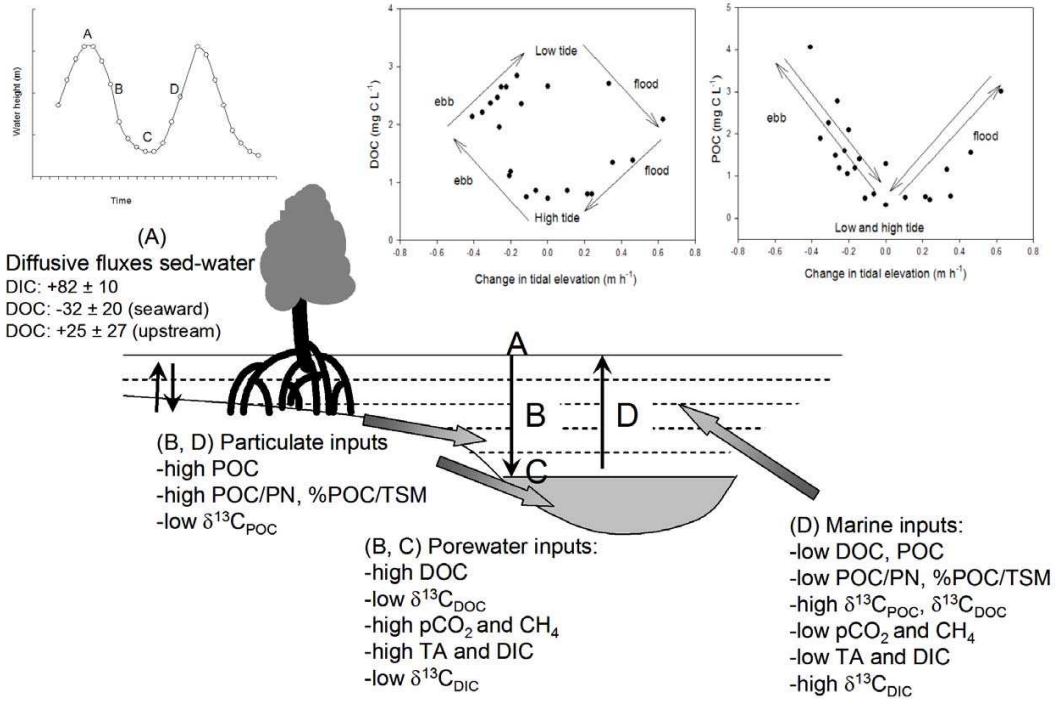


**Fig. 8.** Conceptual scheme of exchange processes for dissolved and particulate matter during a tidal cycle in the tidal creeks. Letters A, B, C, and D refer to high tide, ebb, low tide, and flood, respectively. Fluxes (E. Kristensen, unpublished) are presented in mmol $m^{-2}$ $d^{-1}$, positive fluxes are towards the water column, negative fluxes indicate net uptake by sediments. Middle and right panels at the top show the evolution of DOC and POC, respectively, in the water column during a tidal cycle as a function of the relative change of the water column height.